THE JOURNAL OF BIOLOGICAL CHEMISTRY VOL. 282, NO. 9, pp. 6733–6742, March 2, 2007

Calcium-dependent Regulation of Protein Kinase D Revealed by a Genetically Encoded Kinase Activity Reporter*

Received for publication, August 23, 2006, and in revised form, December 21, 2006 Published, JBC Papers in Press, December 21, 2006, DOI 10.1074/jbc.M608086200

Maya T. Kunkel[‡], **Alex Toker**[§], **Roger Y. Tsien**[‡¶], **and Alexandra C. Newton**[‡1]

From the [‡]*Department of Pharmacology and* [¶]*Howard Hughes Medical Institute, University of California at San Diego, La Jolla, California 92093 and the* [§]*Department of Pathology, Beth Israel Deaconess Medical Center, Harvard Medical School, Boston, Massachusetts 02215*

Protein kinase D (PKD) regulates many diverse cellular functions in response to diacylglycerol. To monitor PKD signaling in live cells, we generated a genetically encoded fluorescent reporter for PKD activity, DKAR (D kinase activity reporter). DKAR expressed in mammalian cells undergoes reversible fluorescence resonance energy transfer changes upon activation and inhibition of endogenous PKD. Surprisingly, we find that agonist-evoked activation of PKD is driven not only by diacylglycerol production, but by Ca^{2+}. Furthermore, elevation of intracellular Ca^{2+}, in the absence of any other stimulus, is sufficient to activate PKD. Concurrent imaging of Ca^{2+}, diacylglycerol, and PKD activity reveals that thapsigargin-mediated elevation of intracellular Ca^{2+} is closely followed by a robust increase in diacylglycerol production, in turn followed by PKD activation. The Ca^{2+}-induced production of diacylglycerol and accompanying PKD activation is dependent on phospholipase C activity. These data reveal that Ca^{2+} is a major contributor to the initiation of PKD signaling through positive feedback regulation of diacylglycerol production, unveiling a new mechanism in PKD activation.

Protein kinase D (PKD)[2] comprises a family of three isoforms belonging to the Ca^{2+}/calmodulin-dependent kinase group of serine/threonine protein kinases. PKD plays a role in numerous processes, including cell proliferation, cell survival, immune cell signaling, gene expression, vesicle trafficking, and neuronal development (1). PKD transduces signals that generate the second messenger diacylglycerol (DAG). This ligand has two roles in the activation of PKD: it activates novel protein kinase C (PKC) family members, which catalyze an activating phosphorylation of PKD, and it directly binds PKD thus recruiting it to the membrane.

PKD isoforms comprise a conserved catalytic core and N-terminal regulatory moiety. The regulatory region contains two cysteine-rich (C1) domains and a pleckstrin homology domain, and this region as a whole acts in an inhibitory manner on the kinase (2). C1 domains are membrane-targeting modules that typically bind DAG and the functional analogues, phorbol esters (3). They are found in a number of proteins, most notably PKC, and provide a mechanism for proteins to be reversibly recruited to membranes in response to DAG. In the case of PKD, binding to either phorbol ester or DAG results in its membrane recruitment and activation.

In addition to membrane recruitment by DAG, activation of PKD requires phosphorylation at two sites within its catalytic core (4). Thus, although DAG production leads to activation of PKD, it is not simply through the C1-mediated membrane binding and removal of autoinhibition by the regulatory region by which PKD becomes active. In addition, the upstream kinases, the novel PKCs, must phosphorylate PKD within its activation loop at Ser-744 and Ser-748 to promote its activity. This phosphorylation event is the rate-limiting step in PKD activation, and once phosphorylated, PKD remains active even after disengaging from DAG (5). Interestingly, the novel PKCs themselves contain C1 domains, so that phorbol ester treatment or DAG production leads to PKD activation through coincident activation of the novel PKCs and localization of PKD near its upstream kinases. Hence, activation of phospholipase C-coupled receptors (such as certain G protein-coupled receptors (GPCRs) or receptor tyrosine kinases) leads to PKD activation via a signaling cascade: stimulation of phospholipase C activity results in the cleavage of the membrane phospholipid phosphatidylinositol bisphosphate to produce the second messengers inositol trisphosphate (IP_3) and DAG. DAG production leads to activation of the novel PKCs, and thus PKD. Although IP_3 stimulates the release of Ca^{2+} from intracellular stores, this consequence of phospholipase C activation is not considered to control PKD activation, because neither the novel PKCs nor PKD bind Ca^{2+}.

To examine PKD signaling in live cells, we generated a genetically encoded fluorescent reporter designed to respond specifically to PKD activity. Such kinase activity reporters generally consist of two different fluorescent proteins flanking a phosphoamino acid-binding domain and a kinase substrate sequence (6–8). Phosphorylation of the substrate sequence causes intramolecular complexation by the phosphoamino

* This work was supported by National Institutes of Health P01 Grants DK54441 (to A. C. N.), CA075134 (to A. T.), and DK07233 (to M. T. K.). The costs of publication of this article were defrayed in part by the payment of page charges. This article must therefore be hereby marked "*advertisement*" in accordance with 18 U.S.C. Section 1734 solely to indicate this fact.

[1] To whom correspondence should be addressed: Dept. of Pharmacology, University of California at San Diego, Leichtag 282, 9500 Gilman Dr., La Jolla, CA 92093-0721. Tel.: 858-534-4527; Fax: 858-822-5888; E-mail: anewton@ucsd.edu.

[2] The abbreviations used are: PKD, protein kinase D; CFP, cyan fluorescent protein; CaMKII, calcium-calmodulin-dependent protein kinase II; DAG, diacylglycerol; DKAR, D kinase activity reporter; FRET, fluorescence resonance energy transfer; PdBu, phorbol 12,13-dibutyrate; PKC, protein kinase C; YFP, yellow fluorescent protein; BAPTA, 1,2-bis(2-aminophenoxy)ethane-*N*,*N*,*N*′,*N*′-tetraacetic acid tetrakis; GPCR, G protein-coupled receptor; IP_3, inositol trisphosphate; DKAR-T/A, DKAR with phospho-acceptor Thr mutated to Ala.

acid-binding domain altering fluorescence resonance energy transfer (FRET) between the fluorescent proteins. The resulting change in FRET enables the visualization of kinase signaling in real time in live cells. Current methods for assaying PKD activation include Western blotting to probe for the activating phosphorylations on PKD and kinase assays of immunoprecipitated PKD. Both of these approaches are effective; however, they can only reveal snapshots of PKD signaling. Design of a genetically encoded fluorescent reporter would allow the monitoring of PKD activity in live cells.

Here we describe the design and use of a PKD reporter, DKAR (D kinase activity reporter), for visualizing agonist-stimulated PKD activation in live cells. We show that DKAR is a sensitive and reversible reporter of endogenous PKD activity. The reporter reveals differences in the kinetics and duration of PKD signaling downstream of distinct GPCRs in two different cell lines; both responses occur rapidly following GPCR stimulation, but in one cell line the signal is sustained whereas in the other cell line the response is transient. Lastly, we show that Ca^{2+} is a major contributor to the agonist-evoked activation of PKD and that it, alone, is sufficient to activate PKD. Visualization of DAG levels reveals that Ca^{2+} stimulates DAG production though positive feedback of phospholipase C, thus accelerating the rate of agonist-induced activation of PKD. In addition, Ca^{2+} can act on its own to stimulate DAG production, thus activating PKD. These data reveal a previously undescribed regulatory input in controlling cellular PKD activity through Ca^{2+}-regulated DAG production.

EXPERIMENTAL PROCEDURES

Materials—Phorbol 12,13-dibutyrate (PdBu), Gö 6983, Gö 6976, thapsigargin, ionomycin, edelfosine (ET-18-OCH_3), and BAPTA/AM were obtained from Calbiochem. KN-93 was obtained from Sigma. Fura 2/AM was obtained from Molecular Probes (Eugene, OR). Antibodies to PKD, to the phosphorylated activation loop of PKD (PKD P-S744/748), to the C-terminal autophosphorylation site of PKD (PKD P-S916), and to phospho-(Ser/Thr) PKD substrates were obtained from Cell Signaling Technology (Beverly, MA). Purified PKD1 (formerly known as PKCμ) was obtained from Upstate. HyBlot CL film used for Western analyses was from Denville Scientific (Plainfield, NJ). All other materials were reagent grade.

Plasmid Constructs—DKAR was generated through substitution of a PKD substrate sequence, LSRQLTAAVSE, for the substrate sequence within C kinase activity reporter (9) by PCR. The phospho-acceptor threonine was mutated to an alanine to create DKAR-T/A following the QuikChange protocol (Stratagene). For *in vitro* experiments, DKAR was subcloned into the bacterial expression vector pRSET B (Invitrogen). MyrPalm-CFP and has been previously described (10). YFP-C1b-Y123W is described in Dries *et al.* (11).

Protein Purification—DKAR and DKAR-T/A were expressed and purified from bacteria as described before (12). In brief, a single colony of BL21(DE3) *Escherichia coli* containing pRSET-DKAR or pRSET-DKAR-T/A was grown for 2 days at room temperature. Pelleted cells were resuspended in 20 mM HEPES, pH 7.5, containing 1 mM dithiothreitol, 300 nM phenylmethylsulfonyl fluoride, 10 μM bestatin, 500 nM benzamidine, and 500 ng/ml leupeptin, and lysed by Dounce homogenization followed by French press. DKAR was purified from cleared lysates by nickel chelation chromatography using nickel-nitrilotriacetic acid-agarose (Qiagen) in the presence of 10 mM imidazole. Following washes, DKAR was eluted in 20 mM HEPES, pH 7.5, 1 mM dithiothreitol containing 200 mM imidazole. Imidazole was removed by dialysis. Protein yield was estimated by CFP absorption at 434 nm.

Kinase Assays—For kinase assays, 1 μg of purified DKAR or DKAR-T/A protein was incubated with 50 units of pure PKD1 or pure PKCβII in a reaction volume of 40 μl at 30°C for 30 min. Buffer compositions were: 50 mM Tris, 2 mM dithiothreitol, 200 μM ATP, 10 mM $MgCl_2$ for PKD and 20 mM HEPES, 2 mM dithiothreitol, 5 mM $MgCl_2$, 200 μM ATP, 500 mM $CaCl_2$, with 140 μM phosphatidyl-serine/3.8 μM DAG vesicles for PKC. Reactions were quenched in sample buffer and analyzed by SDS-PAGE and Western blotting. Blots were probed with the phospho-(Ser/Thr) PKD substrate antibody and analyzed by chemiluminescence using SuperSignal (Pierce).

Cell Transfection—COS-7 and HeLa cells were maintained in Dulbecco's modified Eagle's medium (Cellgro) containing 10% fetal bovine serum and 1% penicillin/streptomycin at 37 °C in 5% CO_2. Cells were plated onto sterilized glass coverslips in 35-mm dishes prior to transfection. Transient transfection was carried out using FuGENE 6 (Roche Applied Science). Cells were imaged within 24 h following transfection.

Cell Imaging—Cells were washed one time in Hanks' balanced salt solution (Cellgro) and imaged in Hanks' balanced salt solution in the dark at room temperature. In pre-treatment experiments, cells were either preincubated with 500 nM Gö 6976 or 250 nM Gö 6983 for at least 10 min, 15 μM BAPTA for at least 15 min at room temperature, 5 μM KN-93 for 20 min at 37 °C, or 10 μM edelfosine for 30 min at 37 °C. Cells were stimulated with: 200 nM PdBu, 100 μM UTP, 10 μM histamine, 5 μM thapsigargin, or 1 μM ionomycin where indicated. Data were collected on a Zeiss Axiovert microscope (Carl Zeiss Microimaging, Inc.) using a MicroMax digital camera (Roper-Princeton Instruments) controlled by MetaFluor software (Universal Imaging Corp.). All optical filters were obtained from Chroma Technologies. Data were collected through a 10% neutral density filter. CFP and FRET images were obtained every 15 s through a 420/20 nm excitation filter, a 450 nm dichroic mirror, and a 475/40 nm or 535/25 emission filter for CFP and FRET, respectively. A YFP image was obtained as a control for photobleaching through a 495/10 nm excitation filter, a 505 nm dichroic mirror, and a 535/25 nm emission filter. Excitation and emission filters were switched in filter wheels (Lambda 10-2, Sutter). Integration times were 200 ms for CFP and FRET and 100 ms for YFP. For Ca^{2+} imaging, COS-7 cells were incubated with Fura-2 AM for 30 min at 37 °C and washed two times with saline prior to imaging. Data were collected every 10 s through a 10% neutral density filter. Images were obtained through a 350/10 nm and a 380/10 nm excitation filter, a 450 nm dichroic mirror, and a 535/45 nm emission filter.

Western Blotting—COS-7 or HeLa cells were grown to confluency in 60-mm dishes. Cells were washed once in Hanks' balanced salt solution and then treated for the indicated times with PdBu, UTP (COS-7 cells), or histamine (HeLa cells) in

Hanks' balanced salt solution at room temperature as shown. Cells were lysed in 50 mM Na_2HPO_4, 1 mM $Na_4P_2O_7$, 20 mM NaF, 2 mM EDTA, 2 mM EGTA, 1% Triton X-100 (supplemented with 1 mM dithiothreitol, 200 μM benzamidine, 40 μg ml^{-1} leupeptin, 300 μM phenylmethylsulfonyl fluoride, and 1 μM microcystin) and cleared by a high speed spin. The cleared lysates were analyzed by Western blotting to determine the relative amounts of PKD S744/748 (activation loop) and PKD S916 (autophosphorylation) phosphorylation. Western blots were developed using chemiluminescence.

RESULTS

Design of DKAR—We have designed a genetically encoded fluorescent reporter, DKAR, to monitor the kinetics of PKD-catalyzed phosphorylation in live cells. This reporter maintains the same modular structure as the previously described PKA, Akt/protein kinase B, and PKC activity reporters, A kinase activity reporter, B kinase activity reporter, and C kinase activity reporter, respectively (9, 12, 13). The primary distinction is that the substrate phosphorylation sequence was modified to make it a phosphorylation sequence for PKD. Specifically, DKAR consists of the FRET pair mCFP (cyan fluorescent protein rendered monomeric by the mutation A206K) and mYFP (the yellow fluorescent protein citrine (14), likewise with A206K) bracketing an FHA2 phosphothreonine-binding domain and a consensus PKD phosphorylation sequence (Fig. 1*A*). The consensus substrate sequence, LSRQLTAAVSE, where the T is the phospho-acceptor residue, was designed based on a combination of data describing optimal PKD phosphorylation consensus sequences and information identifying which residues are critical for FHA2 domain binding (15–18). Analysis of this sequence using Scansite (scansite.mit.edu) suggested that PKD is the preferred kinase to phosphorylate it. As with our previous kinase reporters, unphosphorylated DKAR exists in a conformation resulting in FRET from the donor molecule CFP to the acceptor YFP. Phosphorylation of the threonine within the substrate sequence triggers an intramolecular clamp with the FHA2, leading to a decrease in FRET (Fig. 1*A*).

Phosphorylation of DKAR by PKD in Vitro—To determine whether DKAR can serve as a PKD substrate, DKAR was expressed in bacterial cells as a His-tagged fusion protein, purified, and subjected to *in vitro* phosphorylation by purified PKD. A phosphorylation state-specific antibody, which detects phosphorylations at the optimal PKD sequence motif (15), revealed phosphorylation of DKAR following incubation with the pure kinase (Fig. 1*B*). Importantly, this antibody did not reveal phosphorylation by PKD when a modified DKAR, in which the phospho-acceptor threonine was mutated to alanine (DKAR-T/A), was used. This establishes that PKD specifically phosphorylates the threonine within the designed substrate sequence of DKAR.

Because the phorbol ester PdBu was used to stimulate PKD activity in living cells, we wanted to ensure that PKC, which is potently activated following phorbol ester treatment, was not able to phosphorylate DKAR at the consensus threonine. As seen in Fig. 1*B*, incubation of pure PKCβII with pure DKAR in an *in vitro* kinase assay did not result in phosphorylation of the reporter at the consensus threonine. These results reveal that

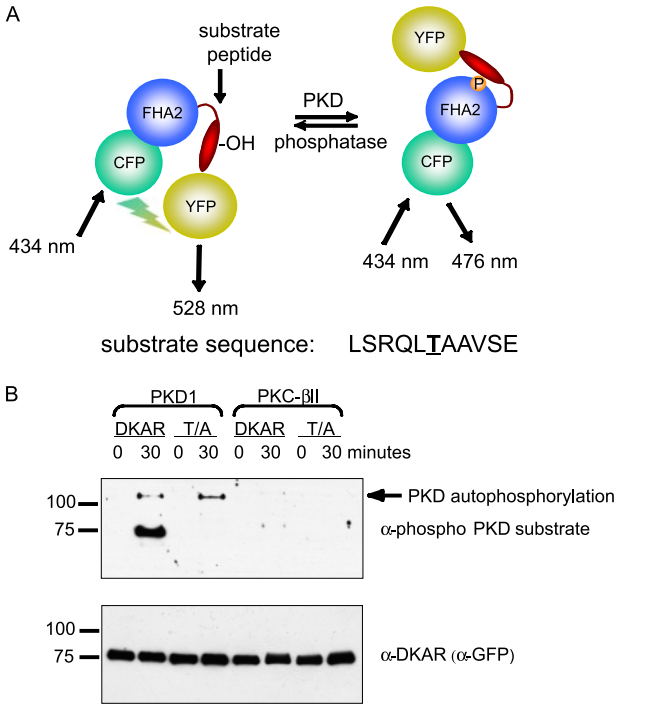

FIGURE 1. **Design of DKAR.** *A*, DKAR consists of mCFP, the FHA2 domain of Rad53, a consensus PKD phosphorylation sequence (*red*), and mYFP. In the unphosphorylated state, mCFP and mYFP are in a proximity and orientation resulting in FRET. Once phosphorylated by PKD at the threonine within the substrate sequence (*underlined*), the FHA2 domain binds the phosphorylated sequence resulting in a conformational change that alters the FRET ratio. *B*, *in vitro* kinase assay monitoring reporter phosphorylation of DKAR or DKAR-T/A (in which the phospho-acceptor site was mutated to Ala) following 30 min of incubation with purified PKD1 or PKCβII. Western blots show phosphorylation detected with the anti-phospho-PKD substrate antibody (*top panel*), and total reporter present was detected with the anti-GFP antibody (*bottom panel*). Autophosphorylation of PKD1 can be observed at the 30-min time point (*arrow*).

PKD, and not PKC, phosphorylates DKAR at the threonine within the substrate sequence.

DKAR Reports PKD Activity in Live Cells—Having demonstrated that pure PKD can recognize and phosphorylate DKAR on the threonine within its substrate sequence *in vitro*, we next wanted to test the ability of DKAR to function as a reporter to visualize PKD signaling in living cells. COS-7 cells overexpressing both DKAR and PKD1 were analyzed following PdBu stimulation. In Fig. 2*A*, the ratio of cyan emission to yellow emission (FRET ratio) was monitored for a few minutes to establish a baseline FRET ratio before stimulating with PdBu. Following PdBu treatment, the FRET ratio increased reflecting the conformational change induced by phosphorylation of the reporter at the consensus threonine. The phospho-acceptor mutant DKAR (DKAR-T/A) did not undergo a FRET ratio change in response to PdBu, confirming that the FRET ratio change results from phosphorylation of the threonine in the designed substrate sequence (Fig. 2*A*).

To test whether DKAR is able to report PKD signaling mediated by endogenous PKD, we expressed only DKAR in COS-7 cells and monitored the FRET ratio change following stimulation with PdBu. PdBu treatment caused the FRET ratio to increase, however, the rate of increase was slower than that observed when PKD was overexpressed (half-time of ~7 min compared with 2 min), and the magnitude of the change was

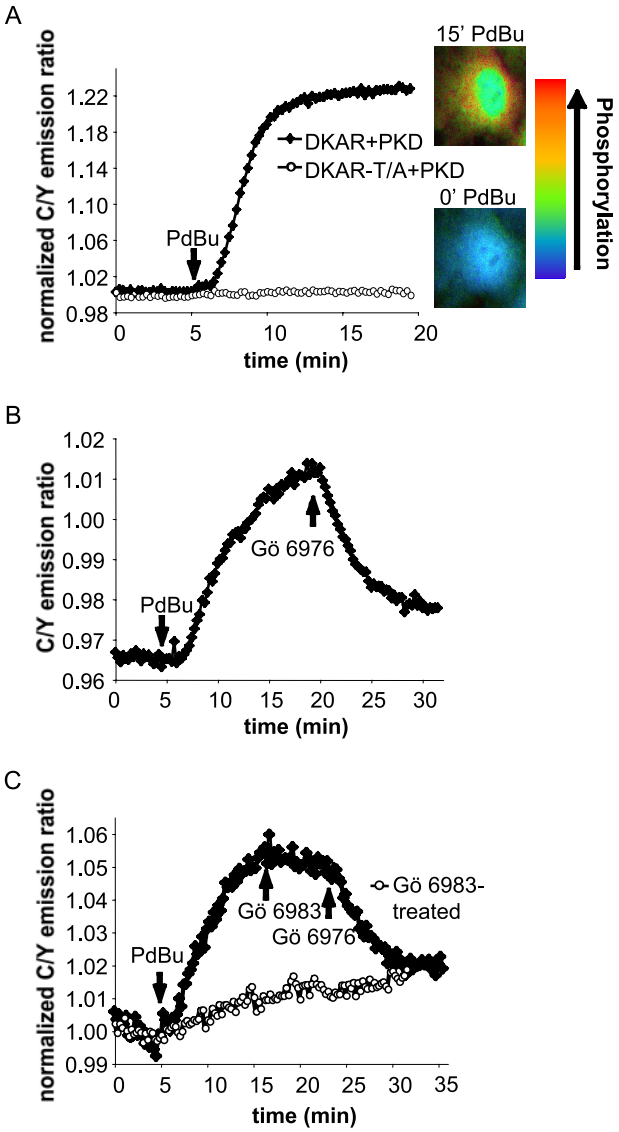

FIGURE 2. **DKAR reversibly reports signaling by PKD.** *A*, COS-7 cells overexpressing PKD1 and DKAR or DKAR-T/A (in which the phospho-acceptor site was mutated to Ala) were treated with PdBu (200 nM), and the ratio of *cyan* emission to *yellow* emission was monitored with time. FRET ratios were normalized and plotted over time. Images (*right*) show pseudocolor representations corresponding to the basal and maximal FRET levels where *blue/green* represents unphosphorylated DKAR (0-min PdBu) and *red* reflects phosphorylated DKAR (15-min PdBu). *B*, COS-7 cells expressing DKAR were imaged during stimulation with PdBu and then treated with the PKD inhibitor Gö 6976. *C*, COS-7 cells expressing DKAR were first treated with PdBu and then treated with the PKC inhibitor Gö 6983 followed by treatment with the PKD inhibitor Gö 6976 as indicated (*black diamonds*). COS-7 cells expressing DKAR were pre-treated with Gö 6983 for 5 min, imaged, and then treated with PdBu (*open circles*). FRET ratios were normalized and plotted over time.

lower (0.05 relative unit compared with 0.20, Fig. 2, compare *A* with *B*). Next, the ability of DKAR to reversibly report PKD signaling was examined by subsequently treating the cells with the PKD inhibitor Gö 6976. Following PKD inhibition, the FRET ratio change induced by PdBu treatment reversed (Fig. 2*B*). Not only does the reversibility of the response indicate that DKAR can act as a readout of both kinase activation and deactivation, but this result also confirms the specificity of PKD as the kinase responsible for phosphorylating DKAR. Thus, DKAR is a sensitive, reversible, and specific reporter of PKD signaling.

The specificity of the DKAR response was further confirmed using a distinct pharmacological agent, Gö 6983, that inhibits all PKC isoforms but does not inhibit PKD. Previously we used Gö 6976, which inhibits not only PKD, but also conventional PKC isoforms. Importantly, Gö 6976 does not inhibit the novel PKC isoforms, which catalyze the activating phosphorylation of PKD. Thus, in the following experiments, cells treated with Gö 6983 would prevent the activating phosphorylations on PKD by novel PKCs, and PKD signaling would be blocked. In Fig. 2*C* (*black diamonds*), cells were treated first with PdBu and monitored until the DKAR FRET ratio reached its maximal response. Subsequent addition of Gö 6983 caused a modest drop in the FRET ratio. Note that this small decline is an artifact resulting from emission of the red-colored inhibitor into the FRET channel,[3] and a similar decline can be observed following Gö 6983 addition in unstimulated cells. Taking this into account, Gö 6983 did not significantly reverse the DKAR response. Only after subsequent addition of Gö 6976 did the FRET ratio reverse. On the other hand, pretreatment of cells for 10 min with the PKC inhibitor Gö 6983 significantly blocked the DKAR response to PdBu (Fig. 2*C*, *open circles*). Together, these results verify the role of the novel PKCs in PKD signaling, and furthermore, they validate the specificity of DKAR as a PKD reporter.

DKAR Reports Signaling Downstream of Endogenous G Protein-coupled Receptors—DKAR was designed to provide a real-time readout of PKD signaling in live cells; therefore, we wanted to monitor DKAR following stimulation of endogenous signaling pathways. To verify that the stimulus used in our study would lead to PKD activation, the phosphorylation state of the activation loop site of PKD was examined following receptor activation. The nucleotide UTP can stimulate phospholipase C-coupled P2Y receptors in many different cell types (19, 20). Treatment of COS-7 cells with PdBu or UTP both resulted in activation of PKD signaling as observed through the induction of phosphorylation of its activation loop site by upstream kinases (Fig. 3*A*). Histamine has been shown to activate G protein-coupled receptors in HeLa cells, and similarly, treatment of HeLa cells with PdBu or histamine resulted in PKD activation as seen by Western analysis of the PKD activation loop sequence (Fig. 3*B*).

Having demonstrated the ability of UTP and histamine to activate PKD in COS-7 and HeLa cells, respectively, we next wanted to examine whether DKAR would report PKD activation following stimulation of these signaling pathways. COS-7 cells expressing DKAR were stimulated with UTP resulting in a rapid and sustained increase in the FRET ratio (Fig. 4*A*). Importantly, pretreatment of COS-7 cells for 10 min with the PKD inhibitor Gö 6976 completely blocked this increase confirming the specificity of DKAR as a reporter for PKD signaling downstream of UTP treatment (Fig. 4*A*). When the consensus threonine within the PKD substrate sequence of DKAR was mutated to an alanine (DKAR-T/A), treatment of cells with UTP resulted in no change in the FRET ratio (Fig. 4*B*). Although PKD signaling in HeLa cells was also observed using DKAR, the

[3] L. L. Gallegos and A. C. Newton, unpublished data.

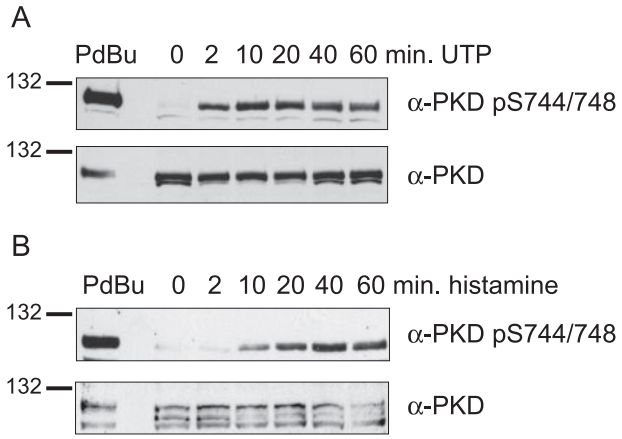

FIGURE 3. **UTP and histamine activate PKD in COS-7 and HeLa cells, respectively.** *A*, lysates from COS-7 cells treated for 10 min with 200 nM PdBu or for the designated times with 100 μM UTP were analyzed by Western blotting for PKD activation using a phospho-specific antibody toward the activation loop of PKD (α-PKD pS744/748). *B*, lysates from HeLa cells treated for 10 min with 200 nM PdBu or for the designated times with 10 μM histamine were analyzed by Western blotting as in *A*.

kinetics of the response was slightly different than the kinetics of the response observed in COS-7 cells following UTP treatment. Specifically, when HeLa cells expressing DKAR were stimulated with histamine, the FRET ratio change observed was rapid but began to decay within 2 min (Fig. 4*C*). However, the response did not fully reverse to baseline levels, even after PKD inhibition with Gö 6976 (data not shown). In accordance with this observation, pre-treatment of HeLa cells for 10 min with Gö 6976 followed by treatment with histamine resulted in a slower FRET ratio change that reached the same level as the new baseline observed from histamine treatment alone (Fig. 4*C*). Therefore, there exists either: 1) nonspecific phosphorylation by a distinct, Gö 6976-insensitive kinase, or 2) a pool of PKD within HeLa cells that cannot be inhibited by Gö 6976 treatment, which results in a ~20% of maximal increase in the FRET ratio from DKAR. As a control, histamine did not cause a change in FRET ratio of DKAR-T/A expressed in HeLa cells (Fig. 4*D*). Interestingly, whereas the phosphorylation at the activation loop site on PKD was much more pronounced following PdBu treatment compared with UTP or histamine treatment (see Fig. 3), the kinetics of the DKAR response triggered by these ligands was considerably faster compared with the response triggered by PdBu (compare Fig. 2*B* with 4*A* and 4*C*). In summary, UTP or histamine treatment of COS-7 or HeLa cells, respectively, activates the PKD pathway resulting in a rapid and readily observed FRET ratio change by DKAR in live cells.

Calcium Stimulates DKAR Phosphorylation—DKAR was designed to be a specific reporter of PKD signaling, and analysis of the substrate sequence by Scansite supported this specificity: a medium stringency scan indicates that PKD is the preferred kinase to phosphorylate DKAR. However, Ca^{2+}/calmodulin-dependent protein kinase II (CaMKII) is predicted by Scansite to be the next most likely kinase to phosphorylate the sequence. To examine the possibility that CaMKII activation may result in a FRET ratio change by DKAR, HeLa cells expressing the reporter were treated with the sarcoplasmic/endoplasmic reticulum Ca^{2+}-ATPase pump inhibitor thapsigargin. Thapsigargin treatment leads to an increase in intracellular Ca^{2+}, a condition that would activate CaMKII within the cells. Following thapsigargin treatment of HeLa cells, DKAR displayed a significant and transient increase in the FRET ratio that returned to a new baseline (Fig. 5*A*). To assess whether CaMKII was mediating this Ca^{2+}-induced FRET response from DKAR, we treated HeLa cells with the CaMKII inhibitor KN-93 before adding

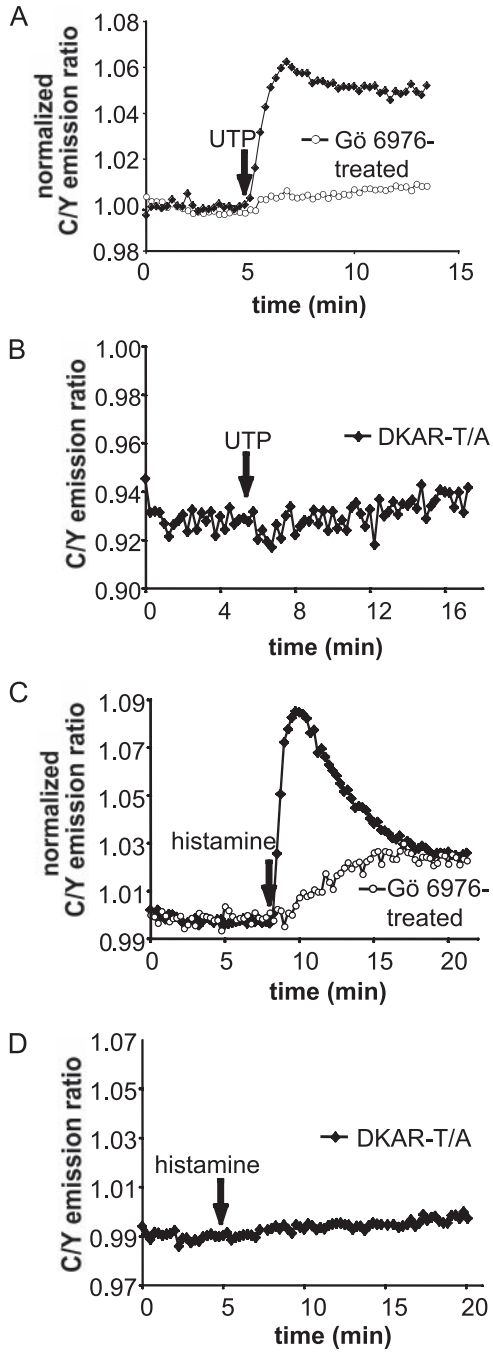

FIGURE 4. **DKAR reports PKD signaling in response to endogenous receptor activation.** COS-7 (*A*) or HeLa (*C*) cells expressing DKAR were treated with UTP or histamine, respectively (*black diamonds*), or pre-treated with Gö 6976 and then treated with UTP or histamine (*open circles*), and the ratio of *cyan* emission to *yellow* emission was monitored with time. FRET ratios were normalized and plotted. COS-7 (*B*) or HeLa (*D*) cells expressing DKAR-T/A were treated with UTP or histamine, respectively.

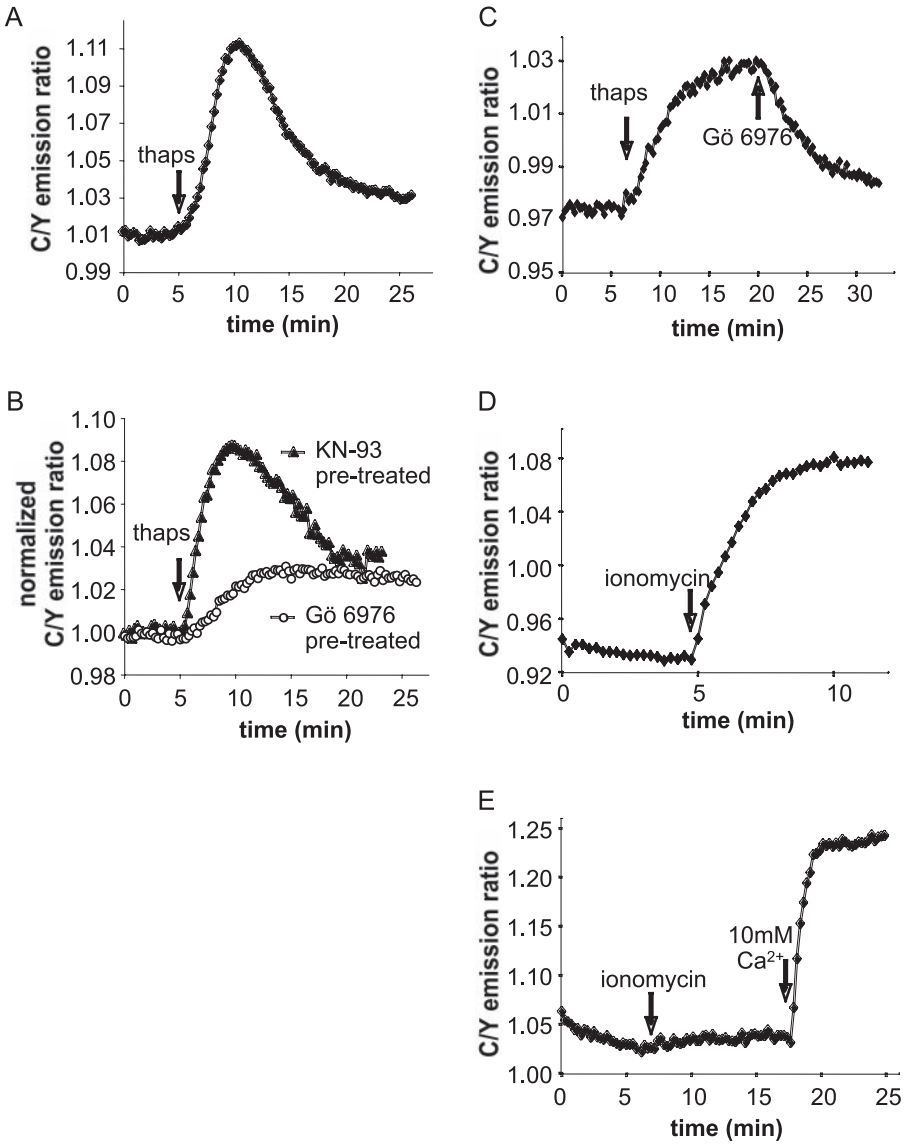

FIGURE 5. **Calcium induces a FRET change from DKAR.** *A*, HeLa cells expressing DKAR were treated with thapsigargin, and the ratio of *cyan* emission to *yellow* emission monitored with time. *B*, HeLa cells expressing DKAR were pre-treated with KN-93 (*black triangles*) or Gö 6976 (*open circles*) and then treated with thapsigargin. FRET ratios were normalized and plotted. *C*, COS-7 cells expressing DKAR were treated with thapsigargin followed by treatment with Gö 6976. *D*, DKAR-expressing COS-7 cells were treated with ionomycin, and the ratio of *cyan* emission to *yellow* emission was monitored with time. *E*, COS-7 cells expressing DKAR were imaged in Ca^{2+}-free saline containing 5 mM EGTA and treated with ionomycin followed by introduction of 10 mM Ca^{2+}.

thapsigargin. As seen in Fig. 5*B* (*closed triangles*), pretreatment of cells with the CaMKII inhibitor KN-93 was not able to block the thapsigargin-induced DKAR FRET ratio change, therefore, CaMKII is not responsible for the FRET change by DKAR following Ca^{2+} release. Instead, pretreatment with the PKD inhibitor Gö 6976 prevented this thapsigargin-induced FRET ratio change (Fig. 5*B*, *open circles*). Because the DKAR response to increasing Ca^{2+} was blocked by Gö 6976 but not KN-93, these data reveal that the Ca^{2+} effect on DKAR is a result of PKD activity not CaMKII activity.

To address whether the activation of PKD by Ca^{2+} is a general phenomenon, we asked whether elevation of Ca^{2+} also regulated PKD activity in a different cell line. Treatment of COS-7 cells with thapsigargin resulted in a slow and sustained FRET ratio change from DKAR that could be reversed to baseline levels following PKD inhibition (Fig. 5*C*). Similar results were observed when Ca^{2+} levels were elevated through a distinct mechanism; COS-7 cells expressing DKAR were treated with the Ca^{2+} ionophore, ionomycin. The FRET ratio of DKAR increased following ionomycin treatment when 1 mM Ca^{2+} was present in the imaging saline (Fig. 5*D*). Removal of extracellular Ca^{2+} along with 5 mM EGTA to chelate residual Ca^{2+} in the imaging saline prevented a FRET ratio increase with ionomycin treatment; however, the FRET ratio increased rapidly when 10 mM Ca^{2+} was added back to the imaging saline (Fig. 5*E*). Thus, surprisingly, increasing Ca^{2+} is sufficient to induce PKD signaling as reported by DKAR.

Increasing Intracellular Ca^{2+} Results in DAG Production—A role for Ca^{2+} in PKD signaling has not been described previously, so our results showing that Ca^{2+} promotes DKAR phosphorylation were unexpected. Activation of PKD has traditionally been observed by monitoring the activating phosphorylations catalyzed by novel PKCs at the activation loop (Ser-744 and Ser-748). Once phosphorylated at these sites, PKD becomes catalytically competent and catalyzes its autophosphorylation at Ser-916 within its C terminus. Thus, this C-terminal site serves as a readout for the intrinsic catalytic activity of PKD. To directly address whether Ca^{2+} activates PKD, we analyzed the phosphorylation state of the activation loop and C-terminal sites of PKD following an increase in intracellular Ca^{2+}. Western blot analyses of PKD from both COS-7 and HeLa cells that were treated for up to 15 min with thapsigargin revealed that PKD is not only phosphorylated by its upstream kinases at the activation loop site, but PKD also autophosphorylates following a rise in intracellular Ca^{2+} (Fig. 6). Thus, as suggested by the DKAR imaging experiments, PKD is activated by increasing Ca^{2+} levels in the cell.

The phosphorylation of the activation loop site on PKD has been reported to be catalyzed by novel PKCs, however, novel PKCs are activated (as is PKD) through the production of DAG, and both novel PKCs and PKD are insensitive to Ca^{2+}. Therefore, the mechanism by which Ca^{2+} triggers the phosphoryla-

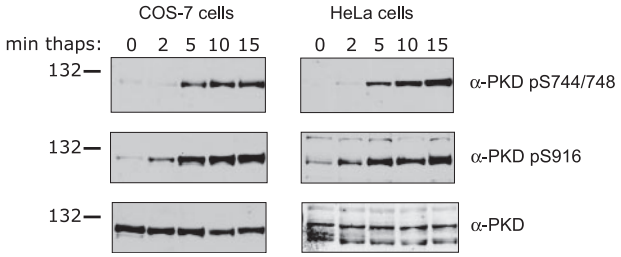

FIGURE 6. **Calcium can activate PKD in COS-7 and HeLa cells.** Lysates from cells treated for the indicated times with thapsigargin were analyzed by Western blotting for PKD activation using an α-PKD pS744/748 antibody (activation loop phosphorylation) and an α-PKD pS916 antibody (autophosphorylation).

tion and activation of PKD cannot be through direct stimulation of novel PKCs or PKD. This led us to ask whether Ca^{2+} could trigger the production of the known upstream messenger DAG. To this end, we employed a FRET-based assay designed in our laboratory that takes advantage of a membrane-tethered CFP (MyrPalm-CFP) domain and a YFP-tagged DAG-binding domain (YFP-C1b-Y123W) (21). Generation of DAG engages the C1 domain on the membrane, resulting in a FRET increase. The DAG-binding domain used was a mutant C1b domain from PKC*β* that was shown to bind DAG with higher affinity than the wild-type C1b domain (11).

We coexpressed MyrPalm-CFP and YFP-C1b-Y123W in COS-7 cells and treated them with thapsigargin to elevate intracellular Ca^{2+}. Thapsigargin caused a robust increase in the FRET ratio between MyrPalm-CFP and YFP-C1b-Y123W (Fig. 7*A*, *black diamonds*), indicating the accumulation of DAG at the plasma membrane. Normalizing to the maximal FRET change evoked by phorbol esters, as described in a previous study (11), revealed that the thapsigargin-induced increase in DAG was on the same order of magnitude as an agonist-evoked increase (data not shown). Thus, one mechanism by which increasing Ca^{2+} leads to activation of PKD is through the production of the second messenger DAG at levels comparable to those elicited by G_q-coupled receptor stimulation. Subsequently, DAG binds and activates both the upstream kinases (the novel PKCs) and PKD itself. To assess whether increasing Ca^{2+} results in the production of DAG via stimulation of phospholipase C activity, we pre-treated cells with the phospholipase C inhibitor edelfosine and then stimulated Ca^{2+} release with thapsigargin. Inhibition of phospholipase C prevented the production of DAG at the plasma membrane following a rise in intracellular Ca^{2+} (Fig. 7*A*, *open circles*).

Having established that Ca^{2+} release results in the production of DAG via phospholipase C activation, we next asked whether the mechanism of the response of DKAR to increasing Ca^{2+} was also through phospholipase C activation. COS-7 cells expressing DKAR were pre-treated with the phospholipase C inhibitor edelfosine and then subsequently stimulated with thapsigargin. In contrast to the results observed in Fig. 5*C*, inhibition of phospholipase C activity with edelfosine completely blocked the DKAR FRET ratio change following thapsigargin treatment (Fig. 7*B*). Thus, increasing intracellular Ca^{2+} leads to phospholipase C activation which, in turn, leads to the production of DAG, which results in the membrane recruitment and activation of both

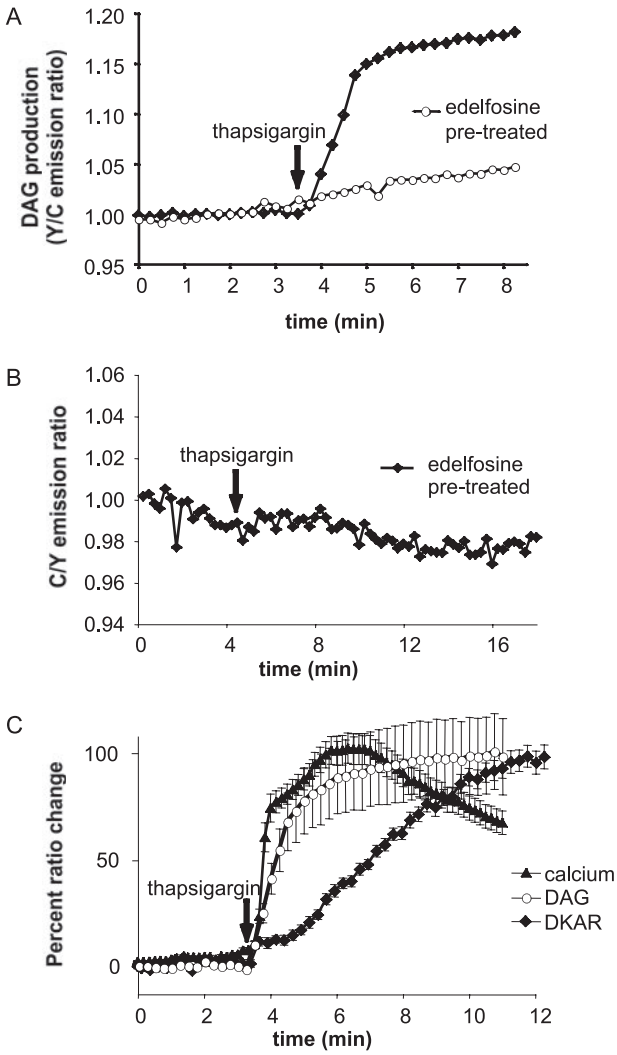

FIGURE 7. **Calcium mobilization activates PKD signaling via the production of DAG at the plasma membrane.** *A*, DAG production was monitored in the absence and presence of the phospholipase C inhibitor edelfosine by analyzing the FRET ratio increase between a YFP-tagged DAG-binding domain and CFP tethered at the plasma membrane in response to thapsigargin treatment. *B*, COS-7 cells expressing DKAR were pre-treated with edelfosine and then treated with thapsigargin while monitoring the FRET ratio. *C*, average Ca^{2+}, DAG, and DKAR responses following thapsigargin treatment were plotted as the percentage of maximal ratio change. Data are the average ± S.E. from at least three different experiments.

the upstream kinases, the novel PKCs, and PKD. Concurrent imaging of intracellular Ca^{2+} levels (Fig. 7*C*, *closed triangles*), plasma membrane DAG (Fig. 7*C*, *open circles*), and activation of PKD as reported by DKAR (Fig. 7*C*, *black diamonds*) revealed that thapsigargin causes a rapid rise in intracellular Ca^{2+} that is closely followed by a robust rise in DAG at the plasma membrane, which is followed by PKD activation.

Calcium Plays a Role in PKD Signaling—Having established that Ca^{2+} increases can lead to production of DAG and thus PKD activation, we were interested in examining the role of Ca^{2+} in the context of PKD signaling downstream of endogenous GPCR activation. To this end, COS-7 cells expressing DKAR were left untreated or pre-loaded with BAPTA (to buffer intracellular Ca^{2+} levels), stimulated with UTP, and the FRET ratio was monitored. Analysis of data from multiple experi-

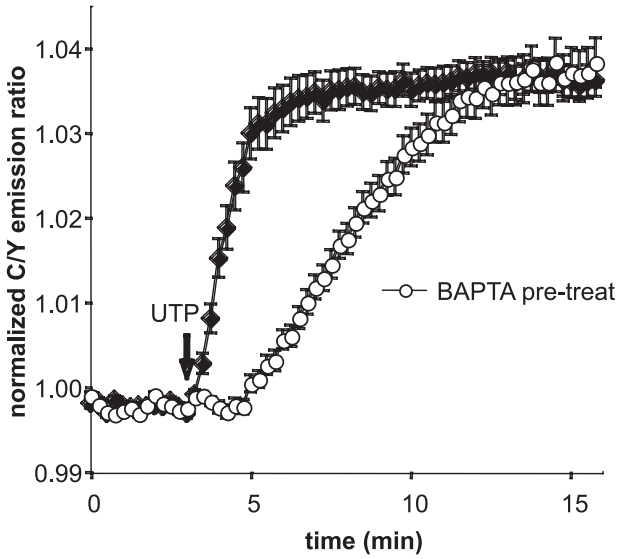

FIGURE 8. **Calcium plays a role in the dynamics of PKD signaling.** COS-7 cells expressing DKAR were stimulated with UTP (*black diamonds*) or pre-loaded with BAPTA for 15 min and then stimulated with UTP (*open circles*), and the ratio of cyan emission to yellow emission was monitored. FRET ratios were normalized and plotted. Data are the average ± S.E. from 9–10 different experiments.

ments ($n \geq 9$) revealed that UTP-stimulated DKAR phosphorylation was delayed by 2 min and then proceeded at a 5-fold lower rate in Ca^{2+}-buffered cells compared with unbuffered cells (Fig. 8). Taken together, these results demonstrate that Ca^{2+} plays a large role in the activation of PKD by regulating the production of DAG.

DISCUSSION

Here we describe the generation and use of DKAR, a novel reporter to visualize PKD activity in live cells. We show that DKAR is a specific, reversible, and sensitive reporter that allows real-time monitoring of activation and deactivation of endogenous PKD signaling. Historically, PKD has been described as being activated downstream of phospholipase C activity, that is, following DAG production at the plasma membrane. However, through the design and characterization of DKAR, we have discovered a novel aspect of PKD signaling: Ca^{2+} drives the rapid activation of PKD. Visualization of DAG levels reveals that Ca^{2+} is sufficient to produce DAG at the plasma membrane thereby activating the PKD pathway. Thus, Ca^{2+} actively participates in PKD signaling by increasing phospholipase C-generated DAG.

Differential Signaling by PKD—The reversibility of DKAR FRET changes reflects the balance between PKD activity and phosphatase activity acting on DKAR within the cell. This reversibility allowed us to examine the kinetics of both signal initiation and signal termination in PKD signaling. We found that the rate of activation was consistently rapid, but the duration of signaling varied among cell types. Specifically, in COS-7 cells, stimulation of cell surface P2Y receptors by UTP results in a rapid and prolonged response by DKAR, whereas in HeLa cells, histamine receptor stimulation causes a fast, but transient response (see Fig. 4). The prolonged *versus* transient nature of PKD signaling downstream of these two distinct G_q-coupled receptors may reflect the differential control of intracellular phosphatases within the two cell types. That is, differences in basal or stimulated phosphatase activity in HeLa compared with COS-7 cells could account for the different rates of signal termination in these two cell types. Consistent with this, the response by DKAR following increases in intracellular Ca^{2+} displayed a similar profile to GPCR stimulation within each cell line: thapsigargin treatment in COS-7 cells resulted in a sustained DKAR response, whereas the response to thapsigargin in HeLa cells was transient. Thus it seems likely that the different responses by DKAR from the two cell types are regulated at the level of cellular phosphatase activity and downstream of the G proteins or GPCRs.

Interestingly, the rate of the DKAR response to G_q-coupled receptor activation (by UTP in COS-7 cells or histamine in HeLa cells) is much faster than that observed following PdBu stimulation or thapsigargin treatment. This is not a reflection of slower incorporation of PdBu into membranes, because we routinely observe rapid (15–30 s) translocation of C1 domains to all membranes following PdBu addition (21), nor is this a reflection of a delay in the Ca^{2+} increase by thapsigargin as Ca^{2+} increases maximally within 15 s of drug addition (Fig. 7). Rather, this faster response may be because PKD is not simply diffuse throughout the cell, but rather, PKD is pre-localized to scaffolds within the cell. Carnegie and colleagues (22) have demonstrated that PKD can exist at a signaling scaffold termed AKAP-Lbc, which pre-localizes PKD and its upstream kinase along with a number of other proteins. Thus, potential pre-localization of PKD to a scaffold containing the upstream kinase at or near the respective G_q-coupled receptor could account for the rapid DKAR response observed following receptor stimulation that is not seen following PdBu treatment or Ca^{2+} mobilization alone. It is also tempting to speculate that activation of G_q-coupled GPCRs leads to an acute inhibition of local phosphatases; this would explain why we observe a much faster DKAR response following GPCR stimulation compared with PdBu or thapsigargin treatment. Consistent with this, we have shown that phosphatases are highly active in the cell under resting conditions (21). Thus, stimulation of GPCRs may lead to temporary inhibition of their activity to enhance the effect of kinases activated downstream thereby leading to a more rapid response from DKAR.

Calcium Regulates PKD—During the characterization of DKAR as a PKD reporter, the ability of Ca^{2+} to trigger the production of DAG and hence activate PKD was revealed. Initially we had sought to address the possibility that CaMKII might be able to phosphorylate DKAR, and, in fact, following Ca^{2+} release from intracellular stores using thapsigargin, we observed a very clear FRET ratio change from DKAR. However, a CaMKII inhibitor had no effect on this response; only following the addition of the PKD inhibitor were we able to block or reverse the thapsigargin-induced FRET ratio increase (Fig. 5). Thus the pharmacological evidence suggested that the Ca^{2+}-induced FRET ratio change of DKAR was the result of PKD phosphorylation on the reporter. Examination of the phosphorylation state of PKD (a readout of its activation state) confirmed the finding that the observed DKAR response was indeed a result of PKD activation. These results were surprising,

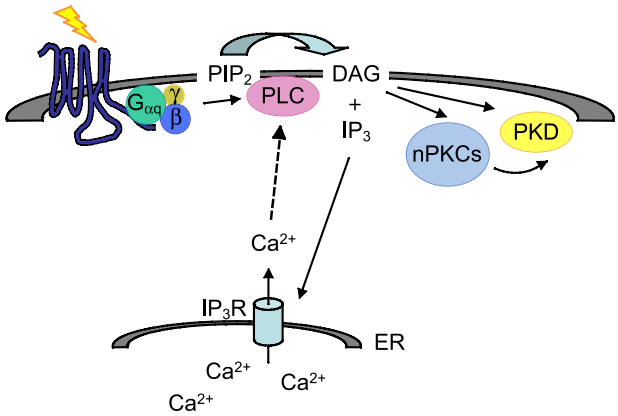

FIGURE 9. **Model describing novel role of Ca^{2+} in PKD activation.** Stimulation of G_q-coupled receptors leads to the activation of phospholipase Cβ, which hydrolyzes phosphatidylinositol bisphosphate (*PIP$_2$*) to form the two second messengers diacylglycerol (*DAG*) and inositol trisphosphate (*IP$_3$*). DAG within the plasma membrane results in the recruitment and activation of the upstream kinases of PKD, the novel PKCs (nPKCs), and PKD itself. IP_3 stimulates the release of Ca^{2+} from intracellular stores. Ca^{2+} can act to positively feedback on phospholipase C activity resulting in increased production of DAG and IP_3. Importantly, Ca^{2+} alone can stimulate production of DAG, presumably through stimulation of phospholipase C activity in the cell (*dotted line*).

because, to date, the critical component in stimulating the PKD pathway downstream of GPCRs has been described as the second messenger DAG, not Ca^{2+}. The upstream kinases of PKD (the novel PKCs) and PKD itself both contain DAG-binding C1 domains that mediate their translocation to the plasma membrane where the novel PKCs are activated and able to phosphorylate their substrates, including PKD. Thus, our finding that Ca^{2+} alone was sufficient to activate phosphorylation of PKD at its activation loop site (the novel PKC site) raised the question of whether Ca^{2+} itself could lead to the production of DAG. Indeed, we verified this by using a FRET-based assay recently designed in our laboratory (11, 21). Using this system, we clearly observed the production of DAG at the plasma membrane in response to increases in intracellular Ca^{2+} (Fig. 7). Thus, the mechanism by which Ca^{2+} activates PKD is still via the production of DAG.

The simplest mechanism by which Ca^{2+} can lead to DAG production would be through direct activation of phospholipase Cs in the cell. Although phospholipase Cβ is the phospholipase activated by G_q-coupled receptors, there are a number of other phospholipase C isozymes that could also confer this response to Ca^{2+}. Indeed binding of Ca^{2+} within their catalytic core is essential for activity of all the phospholipase C isozymes (23). Furthermore, there is a report showing that phospholipase Cδ, but not other phospholipase C subtypes, is responsive to stimulation by rises in intracellular Ca^{2+} (23, 24). Thus it is possible that the activation of PKD through increasing intracellular Ca^{2+} is through direct stimulation of phospholipase C activity.

The observation that Ca^{2+} can activate the PKD pathway has not yet been described. The canonical activator of PKD is DAG. In experiments in the context of the Ca^{2+} chelator BAPTA, the phospholipase C activation by G_q proteins downstream of the GPCRs would remain intact. However, in our experiments, a role of Ca^{2+} on PKD activity was unveiled. Following UTP treatment of COS-7 cells expressing DKAR, where Ca^{2+} levels are maintained below resting levels, we observed an average 2-min delay in PKD activation and 5-fold reduction in rate of activation as reported by DKAR (Fig. 8). Under the Ca^{2+} chelation conditions of our experiments, the G_q protein activated by GPCR stimulation activates phospholipase Cβ, which leads to the production of DAG and IP_3. IP_3 leads to the release of Ca^{2+} from intracellular stores, however, in the presence of BAPTA, this Ca^{2+} response is buffered. It is interesting that the DKAR response is blunted under these conditions. Our results imply that Ca^{2+} is acting within this pathway to regulate phospholipase Cβ. Indeed many studies have described positive feedback by Ca^{2+} on G_q-coupled receptor signaling pathways (25–29). Our findings do not rule out a role of Ca^{2+} released via IP_3 receptor stimulation acting on a distinct phospholipase C subtype, such as phospholipase Cδ, but they confirm a role of Ca^{2+} in regulating DAG production as a whole.

Fig. 9 depicts a model for the proposed role of Ca^{2+} in the PKD activation pathway. Stimulation of G_q-coupled receptors leads to the activation of phospholipase Cβ, which hydrolyzes phosphatidylinositol bisphosphate to form the two second messengers DAG and IP_3. DAG production at the plasma membrane results in the recruitment and activation of PKD, both via translocation and activation of its upstream kinases, the novel PKCs, and through translocation of PKD itself. Once in proximity to the novel PKCs at the membrane, PKD becomes phosphorylated and thereby activated. Concurrently, IP_3 stimulates the release of Ca^{2+} from intracellular stores, and this Ca^{2+} provides positive feedback on phospholipase C activity. This positive feedback control of phospholipase C drives the rapid activation of PKD. Additionally, Ca^{2+} alone can stimulate production of DAG, most likely through direct stimulation of phospholipase C activity in the cell. Thus, Ca^{2+} plays a major role in PKD activation via modulation of phospholipase C activity resulting in the production of the lipid messenger DAG.

Acknowledgments—We thank Jon Violin for initial studies on DKAR and Lisa L. Gallegos for helpful discussions.

REFERENCES

1. Toker, A. (2005) *EMBO Rep.* **6,** 310–314
2. Rykx, A., De Kimpe, L., Mikhalap, S., Vantus, T., Seufferlein, T., Vandenheede, J. R., and Van Lint, J. (2003) *FEBS Lett.* **546,** 81–86
3. Kazanietz, M. G. (2002) *Mol. Pharmacol.* **61,** 759–767
4. Iglesias, T., Waldron, R. T., and Rozengurt, E. (1998) *J. Biol. Chem.* **273,** 27662–27667
5. Rozengurt, E., Rey, O., and Waldron, R. T. (2005) *J. Biol. Chem.* **280,** 13205–13208
6. Sato, M., and Umezawa, Y. (2004) *Methods* **32,** 451–455
7. Zhang, J., Campbell, R. E., Ting, A. Y., and Tsien, R. Y. (2002) *Nat. Rev. Mol. Cell. Biol.* **3,** 906–918
8. Violin, J. D., and Newton, A. C. (2003) *IUBMB Life* **55,** 653–660
9. Violin, J. D., Zhang, J., Tsien, R. Y., and Newton, A. C. (2003) *J. Cell. Biol.* **161,** 899–909
10. Zacharias, D. A., Violin, J. D., Newton, A. C., and Tsien, R. Y. (2002) *Science* **296,** 913–916
11. Dries, D. R., Gallegos, L. L., and Newton, A. C. (2007) *J. Biol. Chem.* **282,** 826–830
12. Kunkel, M. T., Ni, Q., Tsien, R. Y., Zhang, J., and Newton, A. C. (2005)

J. Biol. Chem. **280,** 5581–5587
13. Zhang, J., Ma, Y., Taylor, S. S., and Tsien, R. Y. (2001) *Proc. Natl. Acad. Sci. U. S. A.* **98,** 14997–15002
14. Griesbeck, O., Baird, G. S., Campbell, R. E., Zacharias, D. A., and Tsien, R. Y. (2001) *J. Biol. Chem.* **276,** 29188–29194
15. Döppler, H., Storz, P., Li, J., Comb, M. J., and Toker, A. (2005) *J. Biol. Chem.* **280,** 15013–15019
16. Durocher, D., Taylor, I. A., Sarbassova, D., Haire, L. F., Westcott, S. L., Jackson, S. P., Smerdon, S. J., and Yaffe, M. B. (2000) *Mol. Cell.* **6,** 1169–1182
17. Nishikawa, K., Toker, A., Johannes, F. J., Songyang, Z., and Cantley, L. C. (1997) *J. Biol. Chem.* **272,** 952–960
18. Hutti, J. E., Jarrell, E. T., Chang, J. D., Abbott, D. W., Storz, P., Toker, A., Cantley, L. C., and Turk, B. E. (2004) *Nat. Methods.* **1,** 27–29
19. Brunschweiger, A., and Muller, C. E. (2006) *Curr. Med. Chem.* **13,** 289–312
20. von Kugelgen, I., and Wetter, A. (2000) *Naunyn. Schmiedebergs. Arch. Pharmacol.* **362,** 310–323
21. Gallegos, L. L., Kunkel, M. T., and Newton, A. C. (2006) *J. Biol. Chem.* **281,** 30947–30956
22. Carnegie, G. K., Smith, F. D., McConnachie, G., Langeberg, L. K., and Scott, J. D. (2004) *Mol. Cell* **15,** 889–899
23. Rebecchi, M. J., and Pentyala, S. N. (2000) *Physiol. Rev.* **80,** 1291–1335
24. Allen, V., Swigart, P., Cheung, R., Cockcroft, S., and Katan, M. (1997) *Biochem. J.* **327,** 545–552
25. Horowitz, L. F., Hirdes, W., Suh, B. C., Hilgemann, D. W., Mackie, K., and Hille, B. (2005) *J. Gen. Physiol.* **126,** 243–262
26. Thore, S., Dyachok, O., Gylfe, E., and Tengholm, A. (2005) *J. Cell. Sci.* **118,** 4463–4471
27. Harootunian, A. T., Kao, J. P., Paranjape, S., and Tsien, R. Y. (1991) *Science* **251,** 75–78
28. Eberhard, D. A., and Holz, R. W. (1988) *Trends. Neurosci.* **11,** 517–520
29. Rhee, S. G., Suh, P. G., Ryu, S. H., and Lee, S. Y. (1989) *Science* **244,** 546–550